Vol 463|18 February 2010|doi:10.1038/nature08776

LETTERS

A precision measurement of the gravitational redshift by the interference of matter waves

Holger Müller[1,2], Achim Peters[3] & Steven Chu[1,2,4]

One of the central predictions of metric theories of gravity, such as general relativity, is that a clock in a gravitational potential U will run more slowly by a factor of $1 + U/c^2$, where c is the velocity of light, as compared to a similar clock outside the potential[1]. This effect, known as gravitational redshift, is important to the operation of the global positioning system[2], timekeeping[3,4] and future experiments with ultra-precise, space-based clocks[5] (such as searches for variations in fundamental constants). The gravitational redshift has been measured using clocks on a tower[6], an aircraft[7] and a rocket[8], currently reaching an accuracy of 7×10^{-5}. Here we show that laboratory experiments based on quantum interference of atoms[9,10] enable a much more precise measurement, yielding an accuracy of 7×10^{-9}. Our result supports the view that gravity is a manifestation of space-time curvature, an underlying principle of general relativity that has come under scrutiny in connection with the search for a theory of quantum gravity[11]. Improving the redshift measurement is particularly important because this test has been the least accurate among the experiments that are required to support curved space-time theories[1].

Metric theories of gravity are based on the Einstein equivalence principle (EEP), which states that the local effects of gravity are the same as those of being in an accelerated reference frame. The EEP is derived from three separate experimental observations[1]: the weak equivalence principle (that is, the universality of free fall), local Lorentz invariance, and local position invariance. The first two have been verified experimentally to accuracies of 10^{-13} or better (although some loopholes have not been closed)[1,11]. Local position invariance requires the outcome of a non-gravitational experiment to be independent of where and when it is performed. In practice, the highest-precision tests of local position invariance are measurements of the gravitational redshift: the frequency of an oscillating system (a 'clock') is measured as a function of location. If the EEP holds, there will be no variations other than those caused by gravity, that is, the gravitational redshift.

The basic concept of redshift measurements like ours is to synchronize a pair of clocks when they are located closely to one another, and move them to different elevations. The gravitational redshift will decrease the oscillation frequency of the lower clock relative to the higher one. When we bring the clocks together afterwards and compare the number of elapsed oscillations, there will be a measurable phase shift between them. A famous version of such a measurement was the comparison[7] of atomic clocks in aircraft against ground-based clocks, which confirmed Einstein's prediction with an accuracy of roughly 10%. An accuracy of 7×10^{-5} was obtained by using a hydrogen maser clock in a rocket[8]; 30 years later, this remains the most precise absolute measurement of the gravitational redshift. A higher accuracy of 3.5×10^{-6} is reached by relative redshift measurements[12,13], which verify that there is zero variation between different clocks that move together through space-time. Still, the verification of local position invariance may be called the weakest link in the experimental underpinning of the EEP.

Our determination of the gravitational redshift is based on a reinterpretation of atom interferometry experiments that have been used to measure the acceleration of free fall[9,10,14]. As shown in Fig. 1a, a laser-cooled atom launched vertically upwards in a vacuum chamber is subjected to three pulses from a pair of anti-parallel, vertical laser beams having respective wavenumbers of k_1 and k_2. Each laser pulse transfers the momentum $\hbar(k_1 + k_2)$ (where $\hbar$ is $h/2\pi$, h being the Planck constant) of two photons to the atom (Fig. 1b). The recoil gives a combined momentum impulse of $\hbar k$, where $k \equiv k_1 + k_2$. The intensity and duration of the first laser pulse is adjusted such that this process happens with a probability of 50%. As a result, the first laser pulse places the atom into a coherent superposition of two quantum states, which physically separate owing to their relative momentum $\hbar k$. The second pulse redirects the atom

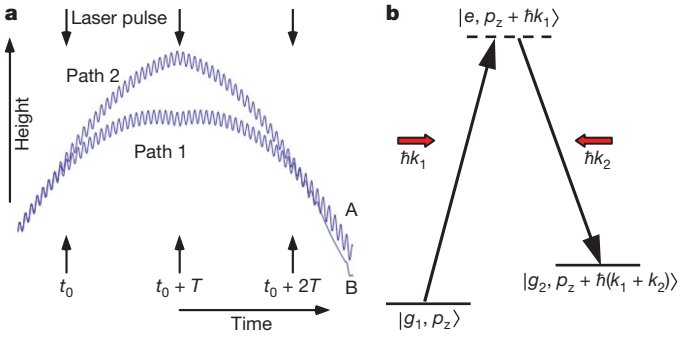

Figure 1 | Atom interferometer and Raman beam splitter. a, Atom interferometer (schematic). The trajectories of the atom are plotted as function of time in the laboratory frame of reference. They are accelerating owing to gravity. The oscillatory lines depict the phase accumulation of the matter waves. Arrows indicate laser pulses applied at times t_0, $t_0 + T$ and $t_0 + 2T$ that change the trajectories. At time t_0, the atom is put into a superposition of two trajectories. At time $t_0 + T$, a laser pulse is used to alter the trajectory of the atoms, and at time $t_0 + 2T$, the phase difference $\Delta\varphi = \Delta\varphi_2 - \Delta\varphi_1$ is recorded. **b**, Two-photon Raman beam splitter. An atom in a quantum state $|g_1, p_z\rangle$, moving upwards with momentum p_z, interacts with photons of two counter-propagating laser beams. The first one transfers the momentum $\hbar k_1$ and brings the atom into a virtual excited state $|e, p_z + \hbar k_1\rangle$. The second laser beam stimulates the atom to emit a photon of momentum $\hbar k_2$, which transfers the atom to another hyperfine ground state $|g_2, p_z + \hbar(k_1 + k_2)\rangle$. With appropriate duration and intensity of the laser pulses, the process can have 50% or 100% probability, creating beam splitters or mirrors for atomic matter waves.

[1]Department of Physics, 366 Le Conte Hall MS 7300, University of California, Berkeley, California 94720, USA. [2]Lawrence Berkeley National Laboratory, One Cyclotron Road, Berkeley, California 94720, USA. [3]Institut für Physik, Humboldt-Universität zu Berlin, Hausvogteiplatz 5-7, 10117 Berlin, Germany. [4]US Department of Energy, 1000 Independence Avenue SW, Washington, District of Columbia 20585, USA.

momentum so that the paths merge at the time of the third pulse (Fig. 1a). More details can be found in the literature[9,10,14].

Quantum mechanics describes the atom on both trajectories as de Broglie matter waves. As they arise from splitting a single wave by the first pulse, their oscillations are initially synchronized. When the waves are superimposed by the third pulse, they may add constructively or destructively, depending on their phase difference, $\Delta\varphi$. The probability of detecting the atom is given by $\cos^2(\Delta\varphi_2 - \Delta\varphi_1)$, where $\Delta\varphi_1$ and $\Delta\varphi_2$ are the total quantum phases accumulated from the beginning of the first laser pulse to the end of the third pulse for each path. By performing the experiment with many atoms and counting them at the two outputs, the probability, and hence the phase difference, is measured. The general relativistic effects on the phase difference $\Delta\varphi_2 - \Delta\varphi_1$ have been calculated in ref. 15 and (within a generalized parameterized post-newtonian[1] test theory) in refs 16 and 17, assuming that local position invariance is valid. As the purpose of our analysis is to study violations of local position invariance, it is useful to re-derive the phase from first principles:

General relativity states that the time measured by a clock moving in curved space-time is given by[18] $\tau = \int \mathrm{d}\tau \equiv \int (-g_{\mu\nu}\mathrm{d}x^\mu \mathrm{d}x^\nu)^{1/2}$. The metric $g_{\mu\nu}$, a 4×4 matrix, describes how this 'proper time' depends on space-time geometry and the location x^μ of the clock. This includes the gravitational redshift and the special relativistic time dilation for a moving clock. The phase accumulation $\Delta\varphi$ of each matter wave is thus given by a free evolution term $\Delta\varphi_{\mathrm{free}}$ and a light–atom interaction term $\Delta\varphi_{\mathrm{light}}$. The term $\Delta\varphi_{\mathrm{free}}$ is given by the elegant expression (see, for example, ref. 18 pages 315–324, and ref. 19)

$$\Delta\varphi_{\mathrm{free}} = \frac{1}{\hbar}\int L\,\mathrm{d}\tau = \frac{1}{\hbar}\int mc^2\,\mathrm{d}\tau = \int \omega_{\mathrm{C}}\mathrm{d}\tau \qquad (1)$$

where L is the Lagrangian and m the mass of the particle. This shows that the phase is the integral of the Compton frequency $\omega_{\mathrm{C}} = mc^2/\hbar$ over the proper time $\mathrm{d}\tau$ as it varies over the trajectory. In Feynman's formulation of quantum mechanics[19], the phase difference is calculated by summing over all possible paths. However, in the case where $\int L\,\mathrm{d}\tau \gg \hbar$, the terms from all paths—except for the extremal path that minimizes the time—cancel. Thus, the above quantum expression requires that the atom fall along the classical, geodesic path.

It is important to emphasize that the oscillation frequency in equation (1) is given by the total energy of the atom, $E = mc^2 = \hbar\omega_{\mathrm{C}}$, which includes the kinetic energy, gravitational energy, internal energy, and most importantly, the rest mass energy. Therefore, this frequency is extremely high (for caesium, for example, $\omega_{\mathrm{C}}/2\pi = 3.2\times10^{25}$ Hz). Although such high frequencies cannot be measured directly, quantum interference provides a means of reading out small phase differences and thus allows us to test fundamental principles in physics to extremely high resolution. Such Compton frequency oscillations have been used, for example, to derive an upper limit to the difference in the gravitational attraction of a K^0 meson and its antiparticle by assuming that the difference in Compton frequencies may be the cause of the conversion of the K-meson known as K_{long} into another K-meson, K_{short} (refs 20, 21). In the analysis of neutrino oscillations, the oscillation frequency includes the rest mass difference of the oscillating neutrinos. An atom interferometer thus provides a textbook test case of general relativity: a neutral atom is almost ideal as a light test particle and contains a built-in quantum clock.

We evaluate equation (1) along the trajectories of the atom. This shows that $\Delta\varphi_{\mathrm{free}} = \Delta\varphi_{\mathrm{redshift}} + \Delta\varphi_{\mathrm{time}}$ is comprised of $\Delta\varphi_{\mathrm{redshift}}$, which is caused by the gravitational redshift, and $\Delta\varphi_{\mathrm{time}}$, which is caused by time dilation because of the velocity of the trajectories (see Methods). We add the light–atom interaction phase $\Delta\varphi_{\mathrm{light}}$, so that $\Delta\varphi = \Delta\varphi_{\mathrm{redshift}} + \Delta\varphi_{\mathrm{time}} + \Delta\varphi_{\mathrm{light}}$ is the sum of three terms. If the gravitational redshift is conventional, it turns out that they have the same magnitude but opposite sign, $\Delta\varphi = \Delta\varphi_{\mathrm{redshift}} = -\Delta\varphi_{\mathrm{time}} = \Delta\varphi_{\mathrm{light}}$ (see Table 1).

To describe measurements of the gravitational redshift, it is common to use the *ansatz*[1] $\Delta\omega = \omega_0(1+\beta)\Delta U/c^2$. Here, $\Delta\omega$ is the change in frequency, ΔU the difference in gravitational potential, and ω_0 is the original frequency of the clock. The parameter β is zero in metric theories of gravity, such as general relativity, regardless of the type of clock[1]. In general, however, different theories can be concocted that differentiate between clocks based on, for example, atomic or nuclear energy levels (which includes combinations of baryon rest mass, electroweak and strong internal energies), kinetic energy, or potential energy.

If the redshift parameter β is non-zero, the phase difference becomes $\Delta\varphi = \Delta\varphi_0(1+\beta)$ (see Table 1 and Methods). Here $\Delta\varphi_0 = kgT^2$ denotes the phase difference[9,10] without redshift anomaly, where g is the local gravitational acceleration and T the pulse separation time (Fig. 1a). This is because $\Delta\varphi_{\mathrm{time}} = -\Delta\varphi_{\mathrm{light}}$ cancel each other and the interferometer phase is equal to the redshift phase, $\Delta\varphi = \Delta\varphi_{\mathrm{redshift}}$. Thus, when k, g and T are known, a measurement of the phase $\Delta\varphi$ is a direct measurement of the redshift.

The most accurate quantum mechanical gravity measurements to date have been performed with an interferometer using caesium atoms in an atomic fountain[9,10]. After correcting for a number of relatively small fundamental[10,17] and systematic[10] effects (Table 1), the redshift is determined from the measured phase $\Delta\varphi$ as $z_{\mathrm{meas}} = \Delta\varphi/(kT^2c^2)$. We find $z_{\mathrm{meas}} = (1.090322683 \pm 0.000000003)\times10^{-16}$ per metre, where the standard error corresponds to a 3 parts per billion accuracy. The acceleration of gravity g varies with space and time owing to gravity gradients and tides. Thus, we used an absolute gravimeter (an FG-5 falling corner cube gravimeter) close by to measure g (corrected for systematic effects, such as elevation, air pressure, tides and polar motion[10]) and determine the locally expected redshift as $z_0 = g/c^2 = (1.090322675 \pm 0.000000006)\times10^{-16}$ per metre. These measurements refer to a particular location (1.810 m above the floor of the laboratory in Stanford, California). However, from the ratio of the measured and expected redshift, we obtain the redshift parameter $\beta = z_{\mathrm{meas}}/z_0 - 1 = (7\pm7)\times10^{-9}$, which is independent of local g and thus a universal constant of gravitation. It is compatible with general relativity within the standard error. This result has been achieved with a pulse separation time T of 160 ms and a peak separation of the trajectories of 0.12 mm. The experiment thus confirms local position invariance by excluding anomalous variations of more than 7 parts in 10^{28} of the frequency of the Compton clocks. This corresponds to comparing the elapsed times to $\sim10^{-29}$ s.

We point out that similar experiments, also based on interference of matter waves, provide a means to verify the gravitational redshift for nanoscale elevations: in Bloch oscillation experiments[22,23], an atomic matter wave interacts with a vertical standing wave of light with a wavelength of λ. This causes periodic potential minima, spaced by $\lambda/2$, for atoms[22,23]. The gravitational redshift of the Compton frequency

Table 1 | Interferometer phase shifts larger than 0.3 p.p.b.

Effect	Equation	Phase shift (rad)
Leading order	$\boldsymbol{(1+\beta)kgT^2}$	**3,698,530.529**
Redshift, $\Delta\varphi_{\mathrm{redshift}}$	$(1+\beta)kgT^2$	
Time dilation, $\Delta\varphi_{\mathrm{time}}$	$-kg'T^2$	
Atom–light interaction, $\Delta\varphi_{\mathrm{light}}$	$+kg'T^2$	
Systematic effects[10]		**−0.018 ± 0.013**
Fundamental effects[17]		
Gravity gradient	$-k\frac{\mathrm{d}g}{\mathrm{d}z}T^3\left[v_{\mathrm{L}}T+\frac{7}{12}gT\right]$	−0.108
Finite speed of light	$3kg^2T^2$	−0.058
Doppler shift	$-3kgv_{\mathrm{L}}T^2$	0.059
First gradient recoil	$-\frac{\hbar k^2}{2m}\frac{\mathrm{d}g}{\mathrm{d}z}T^3$	−0.001
Sum of other effects*		**<0.0001**

Contributions to the interferometer phase, referred to the top of the fountain. The effective wave number k is $2\pi\times2{,}346{,}458.735\,\mathrm{m}^{-1}$, the launch velocity v_{L} is $1.53\,\mathrm{m\,s}^{-1}$, and the gravity gradient $\mathrm{d}g/\mathrm{d}z$ is $-2.9(1)\times10^{-6}\,\mathrm{s}^{-2}$. The gravitational acceleration is denoted g; the actual acceleration g' of the atom may differ slightly, for fundamental or experimental reasons (see Methods).
* See table 1 in ref. 17.

between these locations is $\omega_B = (1+\beta)gm\lambda/(2\hbar)$. This frequency can be observed as an oscillation of the atom's velocity over time. Strontium atoms have been used[22] in an optical lattice of $\lambda/2 = 266$ nm. From the measured frequency, we obtain $\beta = (4.0 \pm 6.0 \pm 0.3) \times 10^{-5}$, where the first standard error is the uncertainty in g (see Methods) and the second the experimental uncertainty. A similar measurement has been reported[23] with rubidium atoms and $\lambda/2 = 394$ nm, which leads to $\beta = (3 \pm 1) \times 10^{-6}$. Here, a more precise value for g was available (ref. 24 and F. Biraben, personal communication). The quoted standard error is statistical because no analysis of systematic errors has been reported. See Fig. 2 for an overview of accuracy and length scale of redshift measurements.

If an anomaly in the gravitational redshift was found, it could turn out to be different for different kinds of clocks. Moreover, as any test of the gravitational redshift operates outside the EEP, we cannot take the universality of free fall for granted. Thus, it may be appropriate to label the redshift parameter β^g_{clock} with two indices that indicate the type of clock and the method used for the measurement of g. Our particular clock is special because its whole rest mass energy mc^2 is used as the clock frequency $mc^2/\hbar$; it is therefore possible that its redshift is different from the one measured with conventional atomic clocks, where the energy of the clock transition contributes only a minuscule portion to the rest mass. Thus, redshift tests with conventional clocks remain interesting, even though the high frequency of our matter wave clocks allows us to reach much higher accuracy. In the context of general relativity, however, the nature of the clock plays no role whatsoever[1], and our matter wave clocks are as good as any other for the purpose of testing the relativistic gravitational redshift.

In summary, we improved the precision of measurements of the gravitational redshift by a factor of 10,000. This compares favourably to the European Space Agency's ACES mission, where it is anticipated that the gravitational redshift can be tested to a precision of 2 p.p.m. (ref. 5). Moreover, the distance scales of our tests (micrometre to millimetre) are strongly different from the kilometre and larger scales of classical tests. Our result improves the overall verification of the EEP by a factor of 500 compared to relative redshift measurements, and by a factor of 10,000 compared to absolute ones.

Our experiment was limited by the uncertainty in g caused by local gravity gradients in our laboratory[9,10]. It should be possible to improve the accuracy 10–100 fold by more precisely mapping the local gravity gradient. Moreover, by using different atom interferometer geometries, upper limits on the validity of different metric theories of gravity can be derived[16]. More sensitive atom interferometers with interferometer paths separated by up to 24 photon momenta have been demonstrated[25,26]. Another increase in the sensitivity can be expected from devices with increased pulse separation times[16], which will also test Einstein's field equations[17]. Also, one can devise different geometries for the trajectories, for which the relative contributions between the redshift, time dilation and interaction phases (see Methods) can be varied.

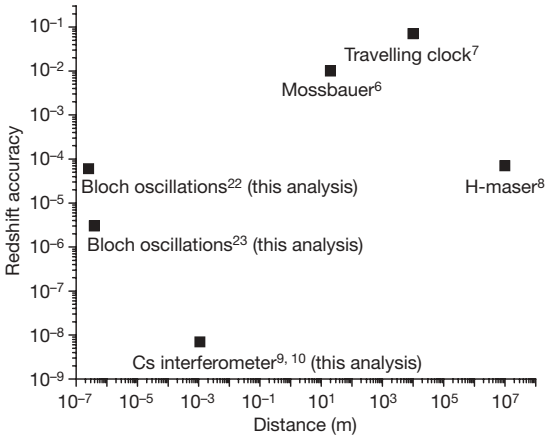

Figure 2 | Absolute determinations of the gravitational redshift. The accuracy (defined as the standard error) in β is plotted versus the relative height of the clocks.

METHODS SUMMARY

The free evolution term $\Delta\varphi_{\mathrm{free}}$ (equation (1)) is evaluated for a central symmetric gravitational field as given by the Schwarzschild metric[18] $g_{\mu\nu}$ with the Earth as central body. We simplify $\Delta\varphi_{\mathrm{free}}$ using the fact that the atom's velocities are much smaller than c and the separation z of the trajectories much smaller than the Earth's radius. We thus obtain $\Delta\varphi_{\mathrm{free}} = \Delta\varphi_{\mathrm{redshift}} + \Delta\varphi_{\mathrm{time}}$ as the sum of two terms, where $\Delta\varphi_{\mathrm{redshift}} = \omega_C \int (gz/c^2)\mathrm{d}t$ is the integral of the gravitational redshift over the trajectory and $\Delta\varphi_{\mathrm{time}}$ is caused by time dilation. In the case of an anomalous gravitational redshift $\Delta\omega = \omega_0(1+\beta)gz/c^2$, where β is the redshift parameter, $\Delta\varphi_{\mathrm{redshift}}$ is modified to $(1+\beta)\omega_C \int (gz/c^2)\mathrm{d}t$. We calculate $\Delta\varphi_{\mathrm{light}}$ using conventional methods[27] and express the phases in terms of the wavenumber k and pulse separation time T. The result (see Table 1) agrees with the non-relativistic calculation[9,10] if $\beta = 0$. This is because in both pictures it is the integral of the gravitational potential energy over time that determines the phase. The essential realization of this Letter is that the non-relativistic formalism hides the true quantum oscillation frequency ω_C. Thus, if we allow for a departure from local position invariance, our analysis shows that the atom interferometer's phase provides a test of general relativity.

It is important to note that, for the interpretation given here, we do not need to know whether the non-standard redshift will lead to modified trajectories of the atom, so long as any such modifications do not significantly change the distance between the interferometer arms. Also, in the case of modified trajectories, tests of the universality of free fall and local position invariance remain conceptually different, as the former search for the variation for different matter at the same location[28], whereas the latter search for effects on similar matter at different locations.

Full Methods and any associated references are available in the online version of the paper at www.nature.com/nature.

Received 21 August; accepted 10 December 2009.

1. Will, C. M. The confrontation between general relativity and experiment. *Living Rev. Relativity* **9**, 3 (2006); ⟨http://relativity.livingreviews.org/Articles/lrr-2006-3/⟩.
2. Ashby, N. Relativity in the global positioning system. *Living Rev. Relativity* 6, 1 (2003); ⟨http://relativity.livingreviews.org/Articles/lrr-2003-1/⟩.
3. Rosenband, T. *et al.* Frequency ratio of Al^+ and Hg^+ single-ion optical clocks; metrology at the 17th decimal place. *Science* **319**, 1808–1812 (2008).
4. Pavlis, N. K. & Weiss, M. A. The relativistic gravitational redshift with 3×10^{-17} uncertainty at NIST, Boulder, Colorado. *Metrologia* **40**, 66–73 (2003).
5. Cacciapuoti, L. & Salomon, C. Space clocks and fundamental tests: the ACES experiment. *Eur. Phys. J. Spec. Top.* **127**, 57–68 (2009).
6. Pound, R. V. & Snider, J. L. Effect of gravity on gamma radiation. *Phys. Rev.* **140**, B788–B803 (1965).
7. Hafele, J. C. & Keating, R. E. Around-the-world atomic clocks: observed relativistic time gains. *Science* **177**, 168–170 (1972).
8. Vessot, R. F. C. *et al.* Test of relativistic gravitation with a space-borne hydrogen maser. *Phys. Rev. Lett.* **45**, 2081–2084 (1980).
9. Peters, A., Chung, K. Y. & Chu, S. A measurement of gravitational acceleration by dropping atoms. *Nature* **400**, 849–852 (1999).
10. Peters, A., Chung, K.-Y. & Chu, S. High-precision gravity measurements using atom interferometry. *Metrologia* **38**, 25–61 (2001).
11. Amelino-Camelia, G., Macias, A. & Müller, H. in *Gravitation and Cosmology* (eds Macias, A., Lämmerzahl, C. & Nuñez, D.) 30 (AIP Conf. Proc. 758, American Institute of Physics, 2005).
12. Fortier, T. M. *et al.* Precision atomic spectroscopy for improved limits on variation of the fine structure constant and local position invariance. *Phys. Rev. Lett.* **98**, 070801 (2007).
13. Blatt, S. *et al.* New limits on coupling of fundamental constants to gravity using ^{87}Sr optical lattice clocks. *Phys. Rev. Lett.* **100**, 140801 (2008).
14. Kasevich, M. & Chu, S. Atomic interferometry using stimulated Raman transitions. *Phys. Rev. Lett.* **67**, 181–184 (1991).
15. Bordé, C. J., Karasiewicz, A. & Tourrenc, Ph General relativistic framework for atomic interferometry. *Int. J. Mod. Phys. D* **3**, 157–161 (1994).
16. Dimopoulos, S., Graham, P. W., Hogan, J. M. & Kasevich, M. A. Testing general relativity with atom interferometry. *Phys. Rev. Lett.* **98**, 111102 (2007).
17. Dimopoulos, S., Graham, P. W., Hogan, J. M. & Kasevich, M. A. General relativistic effects in atom interferometry. *Phys. Rev. D* **78**, 042003 (2008).
18. Misner, C. W., Thorne, K. S. & Wheeler, J. A. *Gravitation* (Freeman, 1970).
19. Feynman, R. P. & Hibbs, A. R. *Quantum Mechanics and Path Integrals* (McGraw-Hill, 1965).
20. Fitch, V. L. The discovery of charge-conjugation parity asymmetry (Nobel Lecture). *Rev. Mod. Phys.* **53**, 367–371 (1981).

21. Good, M. L. K_2^O and the equivalence principle. *Phys. Rev.* **121,** 311–313 (1961).
22. Ivanov, V. V. *et al.* Coherent delocalization of atomic wave packets in driven lattice potentials. *Phys. Rev. Lett.* **100,** 043602 (2006).
23. Cladé, P. *et al.* A promising method for the measurement of the local acceleration of gravity using Bloch oscillations of ultracold atoms in a vertical standing wave. *Europhys. Lett.* **71,** 730–736 (2005).
24. Vitushkin, L. *et al.* Results of the sixth international comparison of absolute gravimeters. *Metrologia* **39,** 407–424 (2002).
25. Müller, H., Chiow, S.-w., Long, Q., Herrmann, S. & Chu, S. Atom interferometry with up to 24-photon-momentum-transfer beam splitters. *Phys. Rev. Lett.* **100,** 180405 (2008).
26. Müller, H., Chiow, S.-w., Herrmann, S. & Chu, S. Atom interferometers with scalable enclosed area. *Phys. Rev. Lett.* **102,** 240403 (2009).
27. Young, B., Kasevich, M. & Chu, S. in *Atom Interferometry* (ed. Berman, P.) 363–406 (Academic, 1997).
28. Dent, Th Eötvös bounds on couplings of fundamental parameters to gravity. *Phys. Rev. Lett.* **101,** 041102 (2008).

Acknowledgements We thank F. Biraben, S.-w. Chiow, S. Herrmann, M. Hohensee, M. Kasevich, G. Tino and P. Wolf for discussions. This material is based on work supported by the National Science Foundation under grants 9320142, 0400866 and 0652332, by the Air Force Office of Scientific Research, and the Department of Energy. H.M. acknowledges support by the David and Lucile Packard Foundation and the National Institute of Standards and Technology under grant 60NANB9D9169. A.P. acknowledges support by the European Science Foundation's EUROCORES program, the European Space Agency, and the German Space Agency DLR (grant DLR 50 WM 0346).

Author Contributions All authors made substantial contributions to this work. The manuscript was written by H.M. and S.C.

Author Information Reprints and permissions information is available at www.nature.com/reprints. The authors declare no competing financial interests. Correspondence and requests for materials should be addressed to H.M. (hm@berkeley.edu).

METHODS

The free evolution term $\Delta\varphi_{\rm free}$, given by equation (1), can be written as

$$\Delta\varphi_{\rm free}=\frac{1}{\hbar}\int L\,{\rm d}\tau=\frac{1}{\hbar}\int mc^2\,\frac{{\rm d}\tau}{{\rm d}t}\,{\rm d}t \qquad (2)$$

so that the integral is now over time coordinate dt. The proper time τ of a clock is given by:

$$c\,{\rm d}\tau=[-g_{\alpha\beta}\,{\rm d}x^{\alpha}{\rm d}x^{\beta}]^{1/2} \qquad (3)$$

For central symmetric gravitational fields, we use the Schwarzschild metric[18]

$$\begin{aligned} g_{tt}&=-(1-\mu/r)c^2,\\ g_{rr}&=1/(1-\mu/r),\\ g_{\theta\theta}&=-r^2,\\ g_{\varphi\varphi}&=-r^2\sin^2\theta, \end{aligned} \qquad (4)$$

where t, r, θ, φ are the time, radius, and angular coordinates, respectively, and $\mu=2GM/c^2$, with G the gravitational constant and M the Earth mass. Then,

$$\begin{aligned} mc^2\frac{{\rm d}\tau}{{\rm d}t}&=\sqrt{-g_{tt}-g_{rr}\dot{r}^2}=mc\sqrt{c^2\left[1-\frac{\mu}{r}\right]-\frac{1}{1-\mu/r}\dot{r}^2}\\ &\approx mc^2\left[1-\frac{1}{2}\left(\frac{\mu}{r_{\oplus}}-\frac{2gz}{c^2}\right)-\frac{1}{2}\left(\frac{\dot{z}}{c}\right)^2\right], \end{aligned} \qquad (6)$$

where $r=r_{\oplus}+z$ with $z\ll r_{\oplus}$, where $r_{\oplus}$ is the radius of the Earth and $g=\mu c^2/(2r_{\oplus}^2)$ the acceleration of free fall at the Earth's surface. In calculating the phase difference between the two paths, the constant terms can be dropped, and we are left with:

$$\Delta\varphi=\frac{1}{\hbar}\int L(z,\dot{z})\,{\rm d}t=-\frac{mc^2}{\hbar}\int\left[\frac{gz}{c^2}-\frac{1}{2}\frac{\dot{z}^2}{c^2}\right]{\rm d}t=-\omega_{\rm C}\int\left[\frac{gz}{c^2}-\frac{1}{2}\frac{\dot{z}^2}{c^2}\right]{\rm d}t \qquad (7)$$

Thus, the free evolution phase shift is given by the integral of the Compton frequency over time, as it is modified by the gravitational redshift gz/c^2 due to the gravitational potential $U=gz$ and by time dilation $\dot{z}^2/(2c^2)$ due to the velocity $\dot{z}$.

For modelling anomalies in the gravitational redshift, we replace the redshift factor by $(1+\beta)gz/c^2$. Equation (7) then becomes:

$$\Delta\varphi=-\omega_{\rm C}\int\left[(1+\beta)\frac{gz}{c^2}-\frac{1}{2}\frac{\dot{z}^2}{c^2}\right]{\rm d}t \qquad (8)$$

By evaluating the integral over the trajectories of the atom and expressing the result in terms of the wavenumber k and the pulse separation time T, we obtain the phases listed in Table 1.

Since the integrals depend on the trajectories of the atom, it might appear necessary to consider whether the physics underlying the violation of local position invariance may also lead to any anomalies in the trajectory of the particle. There is, however, no unique answer. A violation of local position invariance would ultimately be a consequence of refined fundamental laws of physics, such as a version of string theory and loop quantum gravity. No definite version of such a theory, however, exists[11]. Fortunately, it turns out that under some very general assumptions, the interpretation of the redshift test is independent of possible changes in the atom's trajectories. To see this, we consider two scenarios: First, that there is no modification besides the modified gravitational redshift; in particular, that the non-standard value of β does not alter the trajectories. We then evaluate equation (8) and the interaction phase[27] $\Delta\varphi_{\rm light}$ along the standard trajectories. Table 1 shows that the magnitude of the redshift, time dilation, and laser interaction phases are the same if $\beta=0$ and two of these terms cancel each other out. If β is not zero, the time dilation and laser interaction phase still cancel, and the modified redshift directly determines the total phase.

Our second scenario is the more general case that a non-standard value of β does lead to a modified trajectory, which is characterized by a modified acceleration of free fall g'. Such a scenario results, for example, from determining the trajectories by a principle of least action, which states that the trajectories will be the ones for which the phase difference given by equation (8) is lowest. The redshift affects the phase and, therefore, the trajectory. The new trajectory can be derived using the Euler-Lagrange equations. This gives rise to a modified acceleration of free fall g', which, in turn, determines the time dilation and interaction phases. As Table 1 shows, the time dilation and laser interaction phase still cancel, and the result for the total leading-order phase is still directly determined by the redshift. The only assumption we need to make is that any modification due to non-standard physics is common to both trajectories. The relative elevation z, which determines the redshift in equation (8), is then unaffected. This assumption can be expected to hold, because any differential influence should be suppressed by a power of the ratio of the relative velocity or distance of the arms to the velocity and distance scales of the metric, $|(\dot{z}_1-\dot{z}_2)/c|\sim 10^{-10}$ and $|(z_1-z_2)/r_{\oplus}|\sim 10^{-9}$.

We remark that even in the case of modified trajectories, tests of the universality of free fall (UFF) and local position invariance remain conceptually different:[1] Tests of UFF search for the variation for different matter at the same location. For example, the hypothetical modification of trajectories for different matter has been used[28] to derive bounds on the coupling of fundamental constants to gravity. Tests of local position invariance, on the other hand, search for effects on similar matter at different locations.

Thus, the leading-order phase shift is the same in both scenarios,

$$\Delta\varphi=\Delta\varphi_{\rm Path\,2}-\Delta\varphi_{\rm Path\,1}=\frac{mc^2}{\hbar}(1+\beta)\frac{g(\hbar kT/m)T}{c^2}=(1+\beta)kgT^2 \qquad (9)$$

This result is equal to the outcome of the non-relativistic calculation[9,10] if the redshift agrees with general relativity. In particular, equation (7) agrees with the expression of the non-relativistic Lagrangian:

$$\Delta\varphi=-\frac{1}{\hbar}\int[mgz-\frac{1}{2}m\dot{z}^2]\,{\rm d}t=-\frac{1}{\hbar}\int[{\rm PE}-{\rm KE}]\,{\rm d}t \qquad (10)$$

The similarity of the two formalisms when general relativity is valid roots back to the fact that it is the integral of the gravitational potential energy over time $\int U\,{\rm d}t\equiv\int {\rm PE}{\rm d}t$ that determines the accumulated phase due to the redshift U/c^2. The essential realization of this paper is that the non-relativistic equation (10) hides the true quantum oscillation frequency, $\omega_{\rm C}$, given in equation (7). Thus, if we allow for a departure from local position invariance, our analysis shows that the atom interferometer's phase provides a test of general relativity.

Other atom interferometer geometries can also be described in our framework. For example, Ramsey-Bordé interferometers[25,26] have four pulses, at times 0, T, $T+T'$, and $2T+T'$, respectively. The three leading order phases for those are $(1+\beta)kgT(T+T')$ for the redshift, $(\hbar k^2/m)T+kgT(T+T')$ for time dilation, and $-2(\hbar k^2/m)T-kgT(T+T')$ for the laser phase. The sum of these three terms is $-(\hbar k^2/m)T+(1+\beta)kgT(T+T')$.

To estimate g in Florence, Italy, for the experiment ref. 22, we apply the international gravity formula, with corrections for the elevation and the geoid height[29]. To estimate the accuracy of this method, we apply it to four Italian cities for which measurements[30] have been reported and compare prediction and experiment.

29. Lemoine, F. G. *et al. The Development of the Joint NASA GSFC and NIMA Geopotential Model EGM96* (NASA Goddard Space Flight Center, Greenbelt, Maryland, 1998).
30. Fuchs, K. & Soffel, H. in *Landolt-Börnstein – Group V Geophysics* Vol. 2a 317–321 (Springer, 1984).